

University of Arkansas, Fayetteville

ScholarWorks@UARK

---

Civil Engineering Undergraduate Honors Theses

Civil Engineering

---

5-2015

## Evaluation of the Equations Used to Calculate Hydraulic Conductivity Values From Two-Stage Borehole Tests

Johnathon Dale Blanchard  
*University of Arkansas, Fayetteville*

Follow this and additional works at: <https://scholarworks.uark.edu/cveguht>



Part of the [Civil Engineering Commons](#), and the [Hydraulic Engineering Commons](#)

---

### Citation

Blanchard, J. D. (2015). Evaluation of the Equations Used to Calculate Hydraulic Conductivity Values From Two-Stage Borehole Tests. *Civil Engineering Undergraduate Honors Theses* Retrieved from <https://scholarworks.uark.edu/cveguht/22>

This Thesis is brought to you for free and open access by the Civil Engineering at ScholarWorks@UARK. It has been accepted for inclusion in Civil Engineering Undergraduate Honors Theses by an authorized administrator of ScholarWorks@UARK. For more information, please contact [scholar@uark.edu](mailto:scholar@uark.edu), [uarepos@uark.edu](mailto:uarepos@uark.edu).

Evaluation of the Equations Used to Calculate Hydraulic Conductivity  
Values From Two-Stage Borehole Tests

An Undergraduate Honors College Thesis

in the

Civil Engineering  
College of Engineering  
University of Arkansas  
Fayetteville, AR

by

Johnathan Dale Blanchard

**This thesis is approved.**

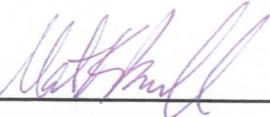
**Thesis Advisor:**



---

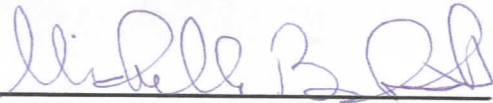
Richard Coffman

**Thesis Committee:**



---

Natalie Becknell



---

Michelle Bernhardt

# Evaluation of the Equations Used to Calculate Hydraulic Conductivity Values From Two-Stage Borehole Tests

Johnathan Blanchard<sup>1</sup>

<sup>1</sup> BSCE Candidate, Department of Civil Engineering, University of Arkansas, Fayetteville AR 72701. jdblanch@uark.edu.

**Abstract:** A compacted clay liner (CCL) test pad was constructed for the purpose of evaluating the testing procedures utilized for determining hydraulic conductivity of a CCL. These procedures include ASTM D6391 (2014) Method C and ASTM D6391 Method A. Method C was recently added to ASTM D6391(2014) and was evaluated based upon comparison of results obtained from previous research with results from the data presented herein. The test pad was instrumented with volumetric water content probes and water matric potential sensors to monitor the wetting front in the soil. The data obtained from this instrumentation should be used to develop a soil water characteristic curve (SWCC) for the soil being tested, and can provide another check for Method C. The effects of pad construction and instrumentation techniques that were utilized discussed. Based on the obtained results Method C is a viable method, but the equation must be corrected prior to use.

**Keywords:** Hydraulic Conductivity, In-situ field testing, Constant Head, Falling Head, Two-Stage Borehole.

## Introduction

Since the mid-1970s there has been a growing emphasis on protecting the environment from exposure to municipal solid waste, prompting new regulations about the way in which municipal waste is disposed of and stored. Many regulations (i.e. Arkansas Regulation Number 22) require landfills to encapsulate municipal waste by using a compacted clay liner (CCL). Typically, a CCL is placed within an acceptable placement window (acceptable water content and corresponding acceptable dry density) that ensures the hydraulic conductivity value (k) for the soil is less than the regulated requirement of  $1E-07$  cm/s. The purpose of this regulation is to limit the amount of leachate that can infiltrate into the groundwater and to ensure adequate shear strength of the clay liner.

These previously developed regulations have successfully improved landfill operations and the impact of landfill facilities on the environment; however, the regulations rely upon the

methods that are used to evaluate and enforce the regulatory requirements. Although numerous papers and research studies have been conducted to examine these methods (e.g. Daniel and Benson 1990, Boutwell and Tsia 1992, Chiasson 2005, Maldonado and Coffman 2012, Nanak 2013) continued research is needed to validate previous results and to evaluate new testing methods. Due to the stringent nature of regulatory requirements and the difficulty of obtaining operating permits, the need for accurate and expedient testing results is paramount.

The constant head test method that is described in ASTM D6391 (2014) Method C was specifically examined, and the results obtained from this method. Moreover, discussion is presented on how the results from newly implemented method (Method C) compare with results from other test methods that have been previously evaluated (Method A and B). Additionally, field scale instrumentation was utilized to enhance the evaluation process and to verify the procedures for measuring the soil water characteristic curve (SWCC) and hydraulic conductivity function (k – functions) that were presented in Ishimwe and Coffman (2015).

The history of the TSB method, relevant research, and other laboratory and field methods are presented in the ‘Background’ section of this document. The ‘Methods and Procedures’ and the ‘Results’ obtained during research are discussed within their respective sections. Finally, the results obtained from this research are presented, and the conclusions and recommendations that are drawn from the results and discussion are presented in the ‘Conclusions and Recommendations’ section.

## **Background**

### **Laboratory Testing**

The way in which regulatory requirements are evaluated varies from state to state. Some states only require the hydraulic conductivity of a landfill liner to be verified through laboratory

testing performed on Shelby tube samples (ASTM D5084 2014), while others require in-situ hydraulic conductivity testing of test sections in addition to laboratory testing performed on Shelby tube samples (ASTM D5084 2014, ASTM D5093 2014, and ASTM D6391 2014). Early discrepancies between field data and laboratory data may be partially responsible for the required field testing in some states. However, Trast and Benson (1995) and Benson et al. (1999) demonstrated that when proper field compaction and low effective stresses (stresses that are similar to field tests stresses) were used in laboratory tests, the hydraulic conductivity values that were calculated from laboratory and field testing methods were similar.

Laboratory testing to determine hydraulic conductivity of field samples is well established. Typical methods include the rigid wall permeameter (RWP) test and the flexible wall permeameter (FWP) test. In the rigid wall test, poor contact between the fine-grained soil and the rigid wall has resulted in hydraulic conductivity values that were artificially high. Therefore, for fine grain soils, like those found in a CCL, a flexible wall permeameter is preferred (ASTM 5084 2014). Utilizing ASTM D5084 (2014), Equations 1-3 are typically used to calculate hydraulic conductivity for a FWP test.

$$k = \frac{a_{in} * a_{out} * L}{(a_{in} + a_{out}) * A * \Delta t} \ln\left(\frac{\Delta h_1}{\Delta h_2}\right) \quad (\text{ASTM D5084, 2014}) \quad \text{Equation 1}$$

$$k_{20} = R_T * k \quad (\text{ASTM D5084, 2014}) \quad \text{Equation 2}$$

$$R_T = 2.2902 * (0.9842^T) / T^{0.1702} \quad (\text{ASTM D5084, 2014}) \quad \text{Equation 3}$$

*In the Equations 1 through 3,  $a_{in}$  is the cross-sectional area of reservoir containing influent/inflow liquid;  $a_{out}$  is the cross-sectional area of the reservoir containing the effluent/outflow liquid;  $L$  is the length of soil sample;  $A$  is the cross-sectional area of soil sample;  $\Delta h_1$  is the head loss across the permeameter at  $t_1$  of water;  $\Delta h_2$  is the head loss across the permeameter at  $t_2$  of water;  $k_{20}$  is the hydraulic conductivity corrected to 20°C (68°F);  $R_T$  is the ratio of viscosity of water at test temperature to viscosity of water at 20°C;  $T$  is an average test temperature during the permeation trial  $((T_1 + T_2)/2)$ ;  $T_1$  is the test temperature at start of permeation trial; and  $T_2$  is the test temperature at end of permeation trial.*

## Field Testing

Two of the methods for determining field hydraulic conductivity values are the TSB method (ASTM D6391 2014) and the sealed double ring infiltrometer (SDRI) method (ASTM D5093 2014). Both of these methods are widely used in industry and are accepted as viable in-situ testing methods (Trautwein and Boutwell 1994). The TSB test was developed in 1983 (Soil Testing Engineers Inc. 1983) by Dr. Gordon Boutwell. Typically, the test is performed according to ASTM D5084 (2014) to measure the flow of water from a standpipe into a borehole at a known time and subjected to a total head. As presented in ASTM D6391 (2014), there are three methods (Method A, B, and C) of evaluating the data obtained from a TSB test. Two stages (Stage 1 and Stage 2) are utilized during Method A while only one stage (Stage 1) is utilized in Methods B and C to determine hydraulic conductivity. A schematic of the different test methods is shown in Figure 1.

Method A, which is a simplified approach to methods proposed by several other authors (Boutwell 1992, Boutwell and Tsai 1992, and Trautwein and Boutwell 1994), was analyzed by Nanak (2013) and was determined to be reasonable method. By following the procedures of Method A, a falling head test is typically performed that generates a K1 and a K2 value (Equations 4 through 10) that are the limiting values for vertical hydraulic conductivity ( $k_v$ ) and horizontal hydraulic conductivity ( $k_h$ ), respectively. To find values for  $k_v$  and  $k_h$ , the anisotropy value ( $m$ ) must be determined. However, determination of this value is not included within the ASTM D6391 (2014) Standard. Soil Testing Engineers Inc. (1983), Daniel (1989), and Trautwein and Boutwell (1994) have all presented methods for finding the anisotropy. The Soil Testing Engineers Inc. (STEI) method was recommended to be used in finding  $k_v$  and  $k_h$  by Nanak (2013); the STEI (1983) equations are presented in Equations 11 and 12.

$$K1 = \frac{R_t G1 \ln\left(\frac{Z1}{Z2}\right)}{(t_2 - t_1)} \quad (\text{ASTM D6391, 2014}) \quad \text{Equation 4}$$

$$K2 = \frac{R_t G2 \ln\left(\frac{Z1}{Z2}\right)}{(t_2 - t_1)} \quad (\text{ASTM D6391, 2014}) \quad \text{Equation 5}$$

$$G1 = \left(\frac{\pi d^2}{11D}\right) \left[1 + a \left(\frac{D}{4b_1}\right)\right] \quad (\text{ASTM D6391, 2014}) \quad \text{Equation 6}$$

$$G2 = \left(\frac{d^2}{16FL}\right) G3 \quad (\text{ASTM D6391, 2014}) \quad \text{Equation 7}$$

$$G3 = 2 \ln(G4) + a \ln(G5) \quad (\text{ASTM D6391, 2014}) \quad \text{Equation 8}$$

$$G4 = \frac{L}{D} + \left[1 + \left(\frac{L}{D}\right)^2\right]^{1/2} \quad (\text{ASTM D6391, 2014}) \quad \text{Equation 9}$$

$$G5 = \frac{\left[\frac{4b_2 + L}{D} + \left[1 + \left(\frac{4b_2 + L}{D}\right)^2\right]^{1/2}\right]}{\left[\frac{4b_2 - L}{D} + \left[1 + \left(\frac{4b_2 - L}{D}\right)^2\right]^{1/2}\right]} \quad (\text{ASTM D6391, 2014}) \quad \text{Equation 10}$$

$$\frac{K2'}{K1'} = m \frac{\ln\left[\frac{L}{D} + \sqrt{1 + \left(\frac{L}{D}\right)^2}\right]}{\ln\left[\frac{mL}{D} + \sqrt{1 + \left(\frac{mL}{D}\right)^2}\right]} \quad (\text{STEL, 1983}) \quad \text{Equation 11}$$

$$K1' = k_v m = \frac{k_h}{m} \quad (\text{STEL, 1983}) \quad \text{Equation 12}$$

*In Equations 4 through 12, d is the internal diameter (ID) of the standpipe; D is the ID of the casing; b<sub>1</sub> is the thickness of the tested soil below the casing; Z<sub>1</sub> is the effective head at the beginning of the time increment; Z<sub>2</sub> is the effective head at the end of the time increment; t<sub>1</sub> is the time at the beginning of the increment(s); t<sub>2</sub> is the time at the end of the increment(s); b<sub>2</sub> is equal to (b<sub>1</sub> – L/2); L is the length of the Stage 2 extension; a is 1 if the base at b<sub>1</sub> is impermeable, 0 for an infinite thickness, and -1 if the base at b<sub>1</sub> is permeable; K1' is the time weighted average for the temporally invariant period for K1; K2' is the time weighted average during the temporally invariant period for K2; and m is determined by using Equation 11 and m is solved for by using the Excel solver function.*

Method A, presented in ASTM D6391 (2014), was developed based on the time lag approach originally proposed by Hvorslev (1951). However, not everyone agreed with this approach. Specifically, Chapuis (1999) has argued that the anisotropy value cannot be



determined and that the assumed flow shape for the borehole was inaccurate. Chapuis (1999) proposed the use of a velocity method instead, which was later altered by Chiasson (2005) to account for scatter in the data when hydraulic conductivity is very small. The Chiasson (2005) method is very similar to Method B in the ASTM (ASTM D6391 2014), which consists of a falling head test that can be used to find a single value for hydraulic conductivity (k) by assuming the soil is isotropic. Method B was also analyzed by Nanak (2013) and found to be technically sound, but returned a much higher value for hydraulic conductivity than other methods. As cited by Nanak (2013), this increase in the value of hydraulic conductivity was attributed to an error in the Chapuis (1999) method. Therefore, Nanak (2013) recommended to not use Method B.

Method C in the ASTM (ASTM D6391 2014) is a constant head test that uses a Mariotte tube to create an air – water interface within the standpipe apparatus and maintain a constant head while the water within the standpipe that surrounds the Mariotte tube decreases with head. This method is required because the changing head in Methods A and B also changes the effective stress, resulting in changes within the measured value of hydraulic conductivity value. Method C was also derived from Hvorslev (1951) but also uses the shape factor presented in Chapuis (1999). The soil is also assumed to be isotropic in Method C. The ASTM D6391 (2014) equation to calculate hydraulic conductivity, using Method C, is presented as Equation 13.

$$k = \frac{\pi(d_s^2 - d_m^2)(Z_1 - Z_2)}{2.75D(k_b)(t_2 - t_1)} \quad (\text{ASTM D5084 2014}) \quad \text{Equation 13}$$

*In Equation 13,  $d_s$  is equal to the ID of the standpipe;  $d_m$  is equal to the outer diameter (OD) of the Mariotte tube;  $Z_1$  is the height of the water in the standpipe at the beginning of the interval(s);  $Z_2$  is the height of the water in the standpipe at the end of the interval(s);  $D$  is the ID of the casing;  $k_b$  is the total head acting on the soil at location of interest;  $t_1$  is the time at the beginning of the increment(s);  $t_2$  is the time at the end of the increment(s).*

The SDRI test was originally developed by Daniel and Trautwein (1986), and is typically performed in accordance with ASTM D5093 (2014) that was based on Trautwein and Boutwell (1994). The SDRI test is conducted by measuring the location of the wetting front and the infiltration rate of water escaping into the soil from a submerged inner ring. Trautwein and Boutwell (1994) proposed three methods of determining  $k$ : the Wetting Front Method, the Suction Head Method, and the Apparent Hydraulic Conductivity Method. The methods vary based on the way in which the hydraulic gradient of the soil is calculated. These methods were evaluated by Nanak (2013) and Ishimwe and Coffman (2015), and yielded similar results to laboratory data and previous TSB testing results.

### **Instrumentation**

Knowing about the location of the wetting front is required for the SDRI test, the use of instrumentation is necessary to assist in the determination about the location of the wetting front. Specifically, tensiometers and water matric potential (WMP) sensors have been used to measure the suction within the soil, which can then be used to determine the location of the wetting front. The suction value is determined using WMP sensors by heating a ceramic (that possesses well defined thermal properties) for a given time and energy. The change in temperature within the ceramic is then used to determine the matric potential ( $\psi$ ) of the soil (Campbell Scientific Inc 2013).

The use of instrumentation to monitor volumetric water content of the soil is also common practice. For instance, time domain reflectometry (TDR) probes have been previously utilized to capture the volumetric water content of the soil ( $\theta_v$ ) by measuring an electric signal as it passes through the soil. Topp et al. (1980) determined that the apparent wavelength, as measured from a probe, could be used to determine volumetric water content (Campbell

Scientific Inc 2013). Furthermore knowledge of the matric suction and the volumetric water content have also allowed for the construction of a soil water characteristic curve (SWCC), as presented in Ishimwe and Coffman (2015).

Through the use of the SWCC, several engineering properties have previously been determined. Specifically, SWCC have been used to determine unsaturated soil properties, which are usually difficult to predict. Therefore, the importance of the SWCC is that the SWCC has been used to determine hydraulic conductivity function ( $k$ -function) for unsaturated soils; which act as an independent in-situ check of the hydraulic conductivity obtained from the field test. Through the use of computer programs like LEACH –M, RETC, UNSAT –H, Vadose/W, and SEEP/W, experimental data have been used to simulate the water movement through the soil, and have successfully been used to define a SWCC (Ishimwe and Coffman 2015) for a given soil.

### **Previous Research Projects**

A considerable amount of research has previously been conducted on CCL performance. Specifically, research conducted at the University of Arkansas by Maldonado and Coffman (2012), Nanak (2013), and Ishimwe and Coffman (2015) has examined the results obtained from the two field testing methods that are commonly used to determine the value of hydraulic conductivity (the TSB and SDRI).

Nanak (2013) evaluated the testing procedures and the methods that can be used to determine a value for hydraulic conductivity from in-situ TSB and SDRI tests, and also investigated the effectiveness of field scale instrumentation (TDR probes and Tensiometers) for determining soil properties during a SDRI test. This was accomplished by comparing field scale hydraulic conductivity data, as collected from a test pad, with laboratory results that were

obtained by conducting FWP tests on samples that were collected from the same test pad. Nanak (2013) performed analysis on three test pads (Test Pad 1, 2, and 3). Test Pads 1 and 2 were evaluated using the TSB method while Test Pad 3 was evaluated using a SDRI.

Ishimwe and Coffman (2015) expanded on the work performed by Nanak (2013) by using field scale instrumentation (TDR probes, WMP sensors, and tensiometers) to generate soil water characteristic curves (SWCC). The testing for Ishimwe and Coffman (2015) was conducted on Test Pad 4, using the SDRI method, and additional instrumentation was utilized to determine the SWCC and the hydraulic conductivity during the SDRI test. This instrumentation also added validity to the soil test results. The conclusion of both of these previously mentioned research studies was that TSB and SDRI tests produce comparable results with laboratory data (within an order of magnitude) and are acceptable methods for determining the hydraulic conductivity of clay within soils that are typically utilized in a CCL. Furthermore, it was concluded that field scale instrumentation should be utilized to enable measurements of the SWCC and  $k$  –functions. However, these measurements should also be confirmed with laboratory measurements on unsaturated soils.

## **Methods and Procedures**

### **Test Pad Construction**

An environmentally-controlled compacted clay liner (test pad) was constructed within the Engineering Research Center (ERC) at the University of Arkansas from June 21 to June 23, 2014. The test pad was constructed within the 10 foot by 10 foot square wooden box that was constructed by Nanak (2013), and was also used by Ishimwe and Coffman (2015). This was the fifth test pad constructed at the University of Arkansas, and is herein after referred to as Test Pad

5. A diagram, outlining the dimensions of the box used to construct the test pad, is presented in Figure 2.

The soil used within the test pad was acquired from the soil stockpile at the ERC that was also used by both Nanak (2013) and Ishimwe and Coffman (2015). This soil was used to make direct comparisons with the results obtained from the previous research. The soil that was used was formerly classified as lean clay in the Unified Soil Classification System and as an A-6(12) in the American Association of State Highway and Transportation Officials (AASHTO) system by Ishimwe and Coffman (2015). The soil was first loaded into a haul bag and was brought into the ERC using a forklift. After unloading the haul bag into the box, the soil was placed using shovels and rakes, the placement procedures are presented in Figure 3.

Four lifts with a nominal thickness of six-inches (eight inch thick loose lifts) of soil were placed; the height of each lift was verified using a surveyor's rod and level. The first two lifts were subdivided into two half lifts (three inch thick compacted lifts and four inch thick loose lifts), each compacted with one-half of the compaction effort. Lift 1 was separated into Lift 1a and 1b, and Lift 2 was separated into Lift 2a and 2b, while Lifts 3 and 4 were compacted as whole lifts. This construction method was used to facilitate the deployment of TDR probes and WMP sensors within these lifts. Following compaction of a half lift, probes were deployed by excavating to the desired probe depth and placing the probes, and then recompacting the soil around the instrumentation using a manual tamper. Following compaction of a bottom portion of the lift (Lift 1a and Lift 2a) and before placement of the top portion of the lift (Lift 1b and 2b), the soil surface was scarred with rakes to increase the cohesion between two half lifts, making the two portions behave more like a continuous lift.

Following the placement of each full thickness lift, the soil was compacted with two passes (one pass for each portion of a divided lift) of a Wacker BS 700 gasoline power rammer. However, the corners and the center of the pad were compacted with a manual tamper. Manual tamping was completed in the corners because the Wacker could not fit into the corners; manual tamping was completed in the center to avoid damage to installed probes. The various compaction techniques that were utilized are presented in Figure 4. This compaction procedure was previously shown by Nanak (2013) to ensure proper compacting of the soil within a placement window that was developed by Nanak (2013). Specifically, the zone of acceptance (ZOA) method was utilized by following the Daniel and Benson (1990). This ZOA was constructed to bound all the acceptable values ( $1 \times 10^{-7}$  cm/s or less) for hydraulic conductivity. To verify proper soil placement, a nuclear density gage was used (ASTM D6938 2014) to collect dry unit weight and water content within each lift at four different locations per lift. The data collected from the nuclear density gage indicated that the soil was over compacted and outside of the placement window, but was still compacted on the wet side of the optimum water content. The nuclear density test locations and the results of the nuclear density testing are presented in Figure 5a and Figure 5b, respectively. After placement and compaction of Layer 4 was completed, the test pad was covered with a plastic cover to prevent loss of moisture content. The pad was constructed to fulfill all of the site requirements that are listed within ASTM D6391 (2014). The pad, after construction and after the plastic cover placement, is presented in the photograph within Figure 6.

### **Instrumentation**

The test pad was instrumented with five Campbell Scientific CS-610 30-centimeter long TDR probes and five Campbell Scientific CS-229 heat dissipation WMP sensors. The probes

were installed in sets (one TDR probe and one WMP sensor). The first three sets were installed at the center of the pad, below the bottom of the maximum depth achieved during Stage 2 of the TSB test. The other two sets were installed below the top of Lifts 3 and Lifts 4 (each centered one foot West of the center of the pad). Each set of probes was installed after first placing and compacting a portioned lift or a full lift and then digging down to install the probe set. A profile view of the probe placement is presented in Figure 7a and plan view is presented in Figure 7b. The TDR probes and WMP sensors were connected to a data acquisition system that collected data automatically every hour. The system consisted of one Campbell Scientific CR-10X, a Campbell Scientific 16 channel AM-416 relay multiplexer, a Campbell Scientific eight channel SDMX-50 multiplexer, and a Campbell Scientific TDR-100 time domain reflectometer. After retrieving the data from the CR-10X with a laptop, the data was processed by using Matlab and Excel.

### **TSB Testing**

The TSB testing was performed in three phases and was conducted in accordance with ASTM D6391 (2014). The first phase of testing was conducted using the constant head test method (Method C), the second phase of testing was conducted using Stage 1 of Method A, and the final phase of testing was conducted using Stage 2 of Method A. Stage 1 of Method A is very similar to Method C, with the only difference being that Method C is conducted with a constant head standpipe (a standpipe with a Mariotte tube). As previously mentioned, Method A has been evaluated and found to be a reasonable method for determining hydraulic conductivity (Nanak 2013). Conversely, as previously mentioned in the 'Background' section and as observed in Ishimwe and Coffman (2015), changing effective stress values (caused by falling head) affect the measured values of hydraulic conductivity of the soil. Therefore, even as Method A was

performed to provide another point of reference for the results from Method C, it is important to note that these results might not be in reference to the same value of total head.

The Stage 1 borehole was excavated using a six-inch diameter hand auger. The base of the borehole was then reamed smooth to a depth of 25.4-centimeters (10 inches) below the top of the soil surface with a six-inch diameter flat bottom auger. To lessen the effects of smearing, the bottom of the borehole was roughened with a wire brush. A four inch ID schedule 40 PVC was then inserted into the borehole and used as the borehole casing. The casing was installed flush with the bottom of the borehole and grouted in place using bentonite pellets. Weights were placed on the top of the casing to prevent uplift during saturation of the bentonite. After 24 hours, the weights were removed and the Method C standpipe apparatus was attached to the top of the casing. Before mounting the standpipe, a nylon sock, filled with pea gravel, was placed into the borehole casing to replace the overburden stress and to prevent scouring of the bottom of the borehole when water was added to the casing.

The standpipe apparatus consisted of a clear PVC tube with a 1.5-centimeter ID that was attached to a four-inch domed PVC cap with the use of PVC cement. The cap had a connection for the water supply, which was located at the cap rather than the top of the standpipe to prevent the accumulation of water along the side of the pipe above the standing water level. There was also a ruler attached to the standpipe with clear tape; the ruler was graduated to the nearest millimeter and was used to measure the height of the water within the tube. A 0.619-centimeter OD clear plastic tube was inserted into the top of the standpipe via an airtight compression fitting that was sealed with epoxy. The end of the tube was open to the atmosphere; effectively becoming the only way for air to enter or exit the system and made the standpipe a Mariotte tube. The standpipe apparatus was attached to the casing with a rubber coupling and hose clamps.



A temperature effects gauge (TEG) was installed using the same procedures utilized to install the TSB, with few modifications. The bottom of the borehole casing was sealed with a flat PVC cap. The tube that was within the standpipe was used to simulate the Mariotte tube, and was sealed at the end with epoxy to prevent water rising up into the tube. The tube was also fed through the top of the standpipe via a non airtight PVC elbow with a rubber stopper at the end to limit the amount of evaporation that occurred. A thermocouple was used to monitor the temperature of the water within the TEG standpipe, and was also fed into the tube via the rubber stopper. A photograph of the assembled TEG and TSB standpipe apparatus is presented in Figure 8 and photographs of the two types of standpipes used in testing are presented in Figure 9.

Method C testing began on July 24, 2014. The tube height of the Mariotte tube was set at 1.7-centimeters above the bottom of the standpipe so as not to exceed the critical gradient and risk hydraulically fracturing the soil. After filling the standpipe, air bubbles were observed to be escaping through the water, implying that the standpipe apparatus was not airtight and the system was currently in a falling head condition. The test was then terminated, and the standpipe apparatus was reassembled, and the test was attempted again. This time the test was determined to be in a constant head condition, but there was too little head to drive the process in a timely manner; therefore, the test was again terminated.

Method C testing recommenced on July 28, 2014, with a new tube height of the Mariotte tube of 15.3-centimeters. This height was chosen to model the head applied during testing by Nanak (2013). Testing continued for 29 days until August 26, 2014, at which point the test was terminated. Per ASTM D6391 (2014) the test was continued past the beginning of the steady state condition, which was determined to have occurred during the second day of testing. However, testing was continued to obtain additional data and to adjust the TEG. The TEG did

not fluctuate as expected, but rather decreased in a slow continuous manner, indicating that the TEG was losing water from an unknown location. After several attempts to correct the problem with the TEG, it was determined that the TEG was still malfunctioning and the TEG data was disregarded. The hydraulic conductivity was evaluated for each time step using the previously presented Equation 13 as obtained from ASTM D6391 (2014), and from Equation 14, which was derived, by the author as a part of this research, from Hvorslev (1951) and Chapuis (1999). The derivation for Equation 14 is presented within Equations 15 through 18; from the derivation it was determined that Equation 14 represents a corrected version of Equation 13.

$$k = \frac{\frac{\pi}{4}(d_s^2 - d_m^2)(Z_1 - Z_2)}{2.75D(k_b)(t_2 - t_1)} \quad \text{ASTM D6391 (2014) modified} \quad \text{Equation 14}$$

$$Q = ckH \quad \text{Hvorslev (1951)} \quad \text{Equation 15}$$

$$k = \frac{Q}{cH} \quad \text{Hvorslev (1951) (rearranged)} \quad \text{Equation 16}$$

$$Q = \frac{AR}{\Delta t} \quad \text{Hvorslev (1951)} \quad \text{Equation 17}$$

$$C = 2.75D \quad \text{Chapuis (1999)} \quad \text{Equation 18}$$

$$\text{Therefore, } k = \frac{Q}{cH} = \frac{\frac{AR}{\Delta t}}{cH} = \frac{AR}{\Delta t cH} = \frac{\frac{\pi}{4}(d_s^2 - d_m^2)(Z_1 - Z_2)}{2.75D(k_b)(t_2 - t_1)}$$

*In Equations 14 through 18,  $d_s$  is equal to the ID of the standpipe;  $d_m$  is equal to the outer diameter (OD) of the Mariotte tube;  $Z_1$  is the height of the water in the standpipe at the beginning of the interval(s);  $Z_2$  is the height of the water in the standpipe at the end of the interval(s);  $D$  is the ID of the casing;  $k_b$  is the total head acting on the soil ( $k_b = H$ );  $t_1$  is the time at the beginning of the increment(s);  $t_2$  is the time at the end of the increment(s);  $A$  is the effective area of the standpipe ( $A = (\pi/4)(d_s^2 - d_m^2)$ ); and  $R$  is the change in height of water in the standpipe ( $R = Z_1 - Z_2$ ).*

After Method C testing was terminated, the Method C standpipe was replaced with the Method A standpipe. Specifically, the Mariotte tube and airtight fitting were replaced with a standpipe that had a PVC elbow joint on the top to prevent evaporation, but allow the standpipe to vent to the atmosphere. Testing for Stage 1 of Method A began August 27, 2014, with a

maximum water elevation of 15 centimeter, which was chosen to model the test performed by Nanak (2013). This testing continued for 40 days until October 6, 2014, at which point Stage 1 was terminated. Again the test was performed well past reaching a state of becoming temporally invariant, which occurred on day two of testing, and was only continued to collect additional data. Method A was evaluated by utilizing Equations 4 through 12 that were previously presented. After the test was terminated, the nylon sock, that was located within the casing, was removed and the water was vacuumed from the borehole. Next, the borehole was extended 15.24-centimeters (six inches). A four-inch bucket and four-inch flat bottom auger were utilized to extend the borehole. After the sides and bottom of the extended borehole were roughened with a wire brush, the nylon sock was again placed into the borehole and the Method A standpipe apparatus were assembled.

Testing for Stage 2 of Method A began October 7, 2014, with the same maximum water elevation that was previously utilized (15 centimeter). Testing continued for 12 days until October 19, 2014, at which point Stage 2 was terminated. The test was performed past the point of reaching a state of becoming temporally invariant, which occurred on day four of testing. However, the test continued until the wetting front reached the bottom of the test pad, as observed in data obtained from the WMP sensors, to ensure the pad was in a steady state flow condition. After the testing was concluded, the standpipes were removed and the pad was prepared for saturation.

### **Saturation**

To determine the drying curve of the SWCC the pad underwent a drying cycle. However, to ensure the complete drying curve was obtained, the pad first underwent a saturation cycle. A hysteresis loop is commonly associated with the SWCC, but due to the range of the WMP

sensors the full saturation curve of the SWCC could not be constructed. Using a 10 foot long 0.25 inch diameter soaker hose spread across the test pad, water was added to the pad for 30 minutes twice a week. The saturation cycle began November 1, 2014, and continued until February 5, 2015. The saturation cycle was originally planned to be terminated when all of the WMP probes indicated that saturation had occurred; however, it was extended until signal interference within the TDR data was eliminated. This delay was required to ensure that the volumetric data obtained during the drying cycle was accurate (without electrical interference) and could be used to construct the drying SWCC.

### **Drying Cycle**

The drying cycle began February 5, 2015 by removing the soaker hose and the plastic that was covering the hose and the pad. Ideally the pad would dry naturally, but to accelerate drying a small box fan was also placed above the northwest corner of the pad. The accelerated drying was due to the time sensitive nature of the project. Unfortunately, this drying process is still ongoing and was not completed at the time of writing this report. Therefore, no RETC or UNSAT –H analysis is included herein.

## **Results and Discussion**

### **Test Pad**

As previously mentioned, the soil used in this project was recycled from previous research projects to enable direct comparison with the previous research. Potential problems with the reuse of the soil include a change in soil structure from previous compaction, an increase in organics and contaminants over time (despite being covered in the stockpile by a geosynthetic), and decreasing supply. With every use some of the soil is wasted due to transportation or because of bentonite contamination from previous SDRI and TSB testing.

Another problem experienced during the construction of Test Pad 5 was the placement of soil being outside of the ZOA. This was attributed to the introduction of half thickness lifts. Although the compaction effort was also decreased (from two passes to one pass for the reduced lifts), all of the tested points in Lifts 1 and 2 were outside of the ZOA (as shown previously in Figure 5b). Conversely, one-half of the test locations within Lift 3 and Lift 4 placed within the ZOA, and the other one-half of the points fell within an area that was not defined by Nanak (2013). Nanak (2013) defined the upper limit for the dry unit weight of the ZOA as 104 pcf; however, Nanak (2013) did not test any points with a dry unit weight between 104 pcf and 105.4 pcf. Consequently, even though several points tested outside the ZOA it is ambiguous as to whether or not the points could have been included in the ZOA. Therefore, more laboratory testing (on points with a dry unit weight between 104 pcf and 105.4 pcf) to better define the ZOA would be useful for further analysis.

Although most of the locations that were using the nuclear density test were located within the portion of the pad that was not used to test hydraulic conductivity (maximum depth achieved at Stage 1 to bottom of the pad [10 inches to 24 inches below the soil surface]) the density at the center of the pad is unknown because no density tests were performed at this location. The center of the pad (where hydraulic conductivity testing took place) could not be tested with the nuclear density gage, because nuclear density tests require a rod to be driven into the soil, which leaves voids in the soil. The center of the pad also underwent a different compaction method (manually tamped), meaning the center of the pad experienced a different compaction effort, making it difficult to correlate acquired test pad densities to the density at the center of the pad.

### **Constant Head Test (Method C)**

Due to the malfunction in the TEG there was more scatter present within the data than there would have been if the TEG had properly functioned. However, the sinusoidal shape of the scatter suggests that the scatter was associated with the effects of varying temperatures. The data was relatively consistent, even with the scatter, and it was relatively easy to select a representative average for the hydraulic conductivity. The coefficient of variation (CoV) of the data collected during the Method C phase of testing was 0.18. However, there was a significant difference (a factor of four) between the average value for hydraulic conductivity obtained using Equation 13 ( $1.43\text{E-}07$  cm/s) and Equation 14 ( $3.58\text{E-}08$  cm/s).

Equation 14 was derived after it was observed that Equation 13 was similar in form to Equation 16, but defined the volume term incorrectly. It was therefore decided that the data should be reduced using both equations for comparison. The average hydraulic conductivity within the temporally invariant period, as calculated using Equation 13 from ASTM D6391 (2014), was found to be  $1.43\text{E-}07$  cm/s. Using the derived Equation 14 the calculated hydraulic conductivity was found to be  $3.58\text{E-}08$  cm/s. The hydraulic conductivity ( $k$ ), as calculated using Equations 13 and 14 for each time step is presented in Figure 10.

The hydraulic conductivity obtained from Method C could not be resolved into vertical and horizontal hydraulic conductivity values because it only utilized the data from Stage 1 of testing and because the soil is assumed to be isotropic (based on the anisotropic construction of the pad, this is a bad assumption). Therefore, hydraulic conductivity values obtained from Method C and from Method A can only be compared in a limited way (Stage 1 data can be compared). Therefore, a shape factor developed for Stage 2 of testing using Method C (constant

head testing) would be a useful tool to analyze the hydraulic conductivity and testing procedures for a CCL.

### **Falling Head Test (Method A)**

The data obtained from the Stage 1 portion of the falling head testing was slightly more scattered than the data collected while following Method C with a CoV equal to 0.23 (as compared to 0.18 during Method C testing). This increase in scatter was likely caused by the nature of the falling head test because the head acting on the soil changed during the test, causing a change in the effective stress and a corresponding change in the hydraulic conductivity. The time dependent relationship created by the changing head can be observed in the data (Figure 10). The data was also susceptible to the effects of varying temperature. However, the data was still reasonably consistent, and was used to find a representative average from the temporally invariant portion of the data. The data collected while following Method A, Stage 1, was variant for the first two days of testing, and then became invariant for the remainder of the test. Similarly, as shown in Figure 10, Stage 2 began as variant and became invariant after seven days of testing.

The average value for  $K_1$ , as determined from Equation 4, was determined to be  $4.88E-08$  cm/s. This value corresponds to the maximum expected value for the vertical hydraulic conductivity. The average value for  $K_2$ , as determined from Equation 5 was determined to be  $1.19E-07$  cm/s. This value corresponds to the minimum value for the horizontal hydraulic conductivity. Using the equations in STEI (1983), presented previously as Equations 11 and 12, and utilizing the Excel Solver function, the  $m$  value was determined to be 5.83. The  $m$  value obtained for this test pad is significantly larger than the  $m$  value as determined by Nanak (2013) for Test Pads 1 and 2, which were 2.19 and 2.39, respectively. This is a consequence of a greater

disparity between K1 and K2 in Test Pad 5 than was observed in Test Pads 1 and 2. The higher m value is an indicator that either the portioned lifts or the instrumentation (these were both absent from Test Pads 1 and 2) caused higher values for horizontal hydraulic conductivity by creating a seam for the water to flow more rapidly. However, the m value was still within the range of reasonable m values according to Casagrande and Poulos (1969). While solving for  $k_v$  and  $k_h$ , based on the average of K1 and K2 and the m value, it was determined that  $k_v$  was equal to  $8.38E-09$  cm/s and  $k_h$  was equal to  $2.85E-07$  cm/s (Figure 10).

### **Comparison of Hydraulic Conductivity Values**

A comparison between the values of hydraulic conductivity obtained from this research and the values of hydraulic conductivity obtained by Nanak (2013) is presented in Table 1. The values for vertical hydraulic conductivity from Stage 1 testing are all within an order of magnitude. Specifically, the average value of K1 from Test Pad 5, Method A ( $4.88E-08$  cm/s), was slightly higher than the average value obtained with the same method on Test Pad 1 ( $1.09E-08$  cm/s) and Test Pad 2 ( $2.18E-08$  cm/s). The increase in the value of hydraulic conductivity was believed to be the result of the increase in the value of pad density observed during pad construction and the difference should be explored more through comparison of soil properties obtained from Test Pad 5 and Test Pads 1 and 2. The value for vertical hydraulic conductivity obtained using the anisotropy (m) value for Test Pad 5 ( $8.38E-09$  cm/s) was also similar in magnitude (within a half order of magnitude) to the same value calculated for Test Pad 1 ( $5.13E-09$  cm/s) and Test Pad 2 ( $9.41E-09$  cm/s).

Method C is also a Stage 1 test, and was compared with values obtained by Nanak (2013) during Stage 1. The values obtained from Method C Stage 1 testing were also larger than the values determined for Method A, Stage 1, testing in Test Pads 1 and 2, but with varying



magnitudes depending on the equation that was used to evaluate the data. The average value calculated using the equation presented by the ASTM D6391 (2014), previously presented as Equation 13 ( $1.43\text{E-}07$  cm/s), was about an order of magnitude greater than the average value determined by Nanak (2013) using the Stage 1 data from Method A. Conversely, the average value ( $3.58\text{E-}08$  cm/s) obtained using the modified equation previously presented in this document as Equation 14 was relatively close to Method A Stage 1 results, being slightly higher than the average value ( $1.09\text{E-}08$  cm/s and  $2.18\text{E-}08$  cm/s for Test Pad 1 and Test Pad 2, respectively) obtained by Nanak (2013) and slightly lower than the K1 average term ( $4.88\text{E-}08$  cm/s) determined for Test Pad 5. This suggests that the modified equation is a better equation (and a more appropriate equation) for determining hydraulic conductivity. Therefore, Equation 14 should be used in testing instead of Equation 13.

The average value obtained during Method A Stage 2 (K2) testing of Test Pad 5 ( $1.19\text{E-}07$  cm/s) was approximately one order of magnitude higher than the values obtained by Nanak (2013) for Test Pad 1 ( $1.50\text{E-}08$  cm/s) and Test Pad 2 ( $3.13\text{E-}08$  cm/s). This disparity was in part attributed to the greater densities observed in Test Pad 5, but was also attributed to the introduction of half lifts and the introduction of probes into the test pad. The value for horizontal hydraulic conductivity obtained using the anisotropy (m) value for Test Pad 5 ( $2.85\text{E-}07$  cm/s) was also approximately one order of magnitude greater than the same value calculated for Test Pad 1 ( $2.52\text{E-}08$  cm/s) and Test Pad 2 ( $5.51\text{E-}08$  cm/s).

### **Instrumentation**

As previously mentioned, during the course of the project, signal interference was observed within the signals from the TDR probes. The interference consisted of a sinusoidal waveform that resonated across the TDR waveform at a high frequency. The high frequency

waveform affected the way in which volumetric water content was calculated, and made the TDR readings very inconsistent. The interference began on August 22, 2014 and progressed until February 5, 2015, at which point the source of the interference was discovered and corrected. The interference was caused by feedback from the laptop that was left connected to the data acquisition system. After discovering the problem, the problem was corrected by disconnecting the laptop between data downloads. Using a Matlab Butterworth Filter the interfering waveform was filtered out, and more consistent volumetric water content data was recovered.

Additional data from the TDR probes and the WMP sensors is still being collected and has not yet been processed by RETC and UNSAT-H. For completeness, the data from the TDR probes and WMP sensors is presented in Figures 11 through 15, for elevations of 0.175 feet, 0.365 feet, 0.48 feet, 1.30 feet, and 1.95 feet above the gravel layer, respectively. Preliminary data from probes and sensors appears to be consistent with data obtained from Ishimwe and Coffman (2015), and it is expected that a well-defined SWCC for each probe set will be developed.

## **Conclusions and Recommendations**

A compacted clay liner (CCL) test pad was constructed for the purpose of evaluating the testing procedure for determining hydraulic conductivity of a CCL that is outlined in the new ASTM D6391 (2014) Method C Standard. Studies evaluating other testing procedures and developing new methods to evaluate these testing procedures, using in-situ instrumentation, were previously conducted by Nanak (2013) and Ishimwe and Coffman (2015), respectively. These results were utilized as the standard for comparison. A two stage borehole (TSB) test was conducted according to ASTM D6391 (2014) Method C and Method A. The average value obtained by using Equation 14 and data from Method C was  $3.58E-08$  cm/s and the data had a CoV of 0.18. The average value obtained by following Method A, Stage 1, was  $4.88E-08$  cm/s, and the data had a CoV of 0.23. The results obtained

by these two methods are similar in value, and suggest that both tests are viable methods for evaluating the hydraulic conductivity of a compacted clay liner.

Volumetric water content probes and soil matric potential sensors were utilized within the pad for the purpose of constructing a soil water characteristic curve (SWCC), according to the procedures proposed by Ishimwe and Coffman (2015). Although the SWCC data are still being collected and the SWCC were not developed the SWCC curves can be used to find a value for hydraulic conductivity to provide another means of comparison for results obtained from Method C. The process of collecting the data to construct a SWCC is currently on going at the time of the writing of this report.

Based on the results obtained from this study (Test Pad 5) the following conclusions and recommendations were obtained.

- A constant head TSB test is a viable method for determining the hydraulic conductivity of a soil.
- The equation used to determine hydraulic conductivity in ASTM D6391 (2014) Method C is incorrectly derived, producing results that are overly conservative by a factor of four.
- The modified equation presented as Equation 14 produces reasonable Data that are consistent with ASTM D6391 (2014) Method A.
- Equation 14 should be used for evaluating data obtained from Method C.
- Data obtained from ASTM D6391 (2014) Method A is susceptible to more scatter than data obtained from ASTM D6391 (2014) Method C, but Method A still provides reasonable results.

- A Stage 2 shape factor should be developed for ASTM D6391 (2014) Method C, this will enhance comparisons with anisotropic tests (Method A).
- The data acquisition of the drying cycle should continue and the SWCC should be developed, as proposed by Ishimwe and Coffman (2015), to provide further comparison with results from ASTM D6391 (2014) Method C.
- Laboratory testing should be conducted to further compare the results obtained from ASTM D6391 (2014) Method C, and to better define the zone of acceptance that was developed by Nanak (2013).

## References

- American Society for Testing and Materials (2014), “Standard Test Method for Measurement of Hydraulic Conductivity of Saturated Porous Materials Using a Flexible Wall Permeameter” Annual Book of ASTM Standards, Designation D 5084, Vol. 4.08, ASTM, West Conshohocken, PA.
- American Society for Testing and Materials (2014), “Standard Test Method for Field Measurement of Infiltration Rate Using Double-Ring Infiltrometer with Sealed-Inner Ring” Annual Book of ASTM Standards, Designation D 5093, Vol. 4.08, ASTM, West Conshohocken, PA.
- American Society for Testing and Materials (2014), “Standard Test Method for In-Place Density and Water Content of Soil and Soil-Aggregate by Nuclear Methods (Shallow Depth)” Annual Book of ASTM Standards, Designation D 6938, Vol. 4.08, ASTM, West Conshohocken, PA.
- American Society for Testing and Materials (2014), “Standard Test Method for Field Measurement of Hydraulic Conductivity Using Borehole Infiltration” Annual Book of ASTM Standards, Designation D 6391, Vol. 4.08, ASTM, West Conshohocken, PA.
- Benson, C., Daniel, D., and Boutwell, G., (1999). “Field Performance of Compacted Clay Liners.” Journal of Geotechnical and Geoenvironmental Engineering, ASCE, Vol. 125, No. 5, pp. 390-403.
- Boutwell, G., (1992). “The STEI Two-Stage Borehole Field Permeability Test.” Containment Liner Technology and Subtitle “D”, Houston Section, ASCE, Houston, TX.
- Boutwell, G. and Tsai, C., (1992). “The Two-Stage Field Permeability Test for Clay Liners.” Geotechnical News, C. Shackelford and D. Daniel, eds., pp. 32-34.
- Campbell Scientific, Inc., (2013a). “TDR Probes CS605, CS610, CS630, CS635, CS640, and CS645.” Instruction Manual. Campbell Scientific Website. Retrieved June 2014.
- Campbell Scientific, Inc., (2013b). “229 Heat Dissipation Matric Water Potential Sensor” Instruction Manual. Campbell Scientific Website. Retrieved June 2014.
- Chapuis, R., (1999). “Borehole variable-head permeability tests in compacted clay liners and covers.” Canadian Geotechnical Journal, Vol. 36, pp. 39-51.
- Chiasson, P., (2005). “Methods of interpretation of borehole falling-head tests performed in compacted clay liners.” Canadian Geotechnical Journal, Vol. 42, pp. 79-90.
- Casagrande, L. and Poulos, S., (1969) “On the effectiveness of sand drains Canadian Geotechnical Journal, 1969, 6(3), 287-326.
- Daniel, D. and Benson, C., (1990). “Water Content-Density Criteria for Compacted Soil Liners.” Journal of Geotechnical Engineering, ASCE, Vol. 116, No. 12, pp. 1811-1830.
- Daniel, D., and Trautwein, S., (1986). “Field Permeability Test for Earthen Liners.” *Proceedings of In Situ '86*, Blacksburg, Va., pp. 146-160.
- Fernando A. M. Marinho (2005). “Nature of soil-water characteristic curve of plastic soils.” Journal of Geotechnical and Geoenvironmental/ Engineering, ASCE. Vol.131, No. 5.

- Hvorslev, J., (1951). "Time Lag and Soil Permeability in Ground Water Observations." Bulletin No. 36, USA/COE WES Vicksburg, MS.
- Ishimwe, E., Coffman, R.A., (2014). "Field-obtained Soil Water Characteristic Curves and Hydraulic Conductivity Functions.". Submitted for Review, Manuscript Number: AGEO- D14-00198
- Maldonado, C., and Coffman, R., (2012). "Hydraulic Conductivity of Environmentally controlled Landfill Liner Test Pad." ASCE Geotechnical Special Publication No. 225, Proc. GeoCongress 2012: State of the Art and Practice in Geotechnical Engineering, Oakland, California, March, pp. 3593-3602.
- Nanak, Matthew J., (2013). "Variability in the Hydraulic Conductivity of a Test Pad Liner System Using Different Testing Techniques." Masters Thesis, University of Arkansas, May 2013.
- Soil Testing Engineers, Inc. (1983). *STEI Two-Stage Field Permeability Test*. Soil Testing Engineers, Inc., Baton Rouge, LA.
- Topp, G., Davis, J., and Annan, A., (1980). "Electromagnetic determination of soil water content: measurements in coaxial transmission lines." *Water Resources Research*, Vol. 16, No. 3, pp. 574-582.
- Trast, J., and Benson, C., (1995). "Estimating Field Hydraulic Conductivity of Compacted Clay." *Journal of Geotechnical and Engineering, ASCE*,
- Trautwein, S. and Boutwell, G. (1994). "In-situ hydraulic conductivity tests for compacted soil liners and caps." *Hydraulic Conductivity and Waste Contaminant Transport in Soil*, STP 1142, D. Daniel and S. Trautwein, eds., ASTM, Philadelphia, pp. 184-223.

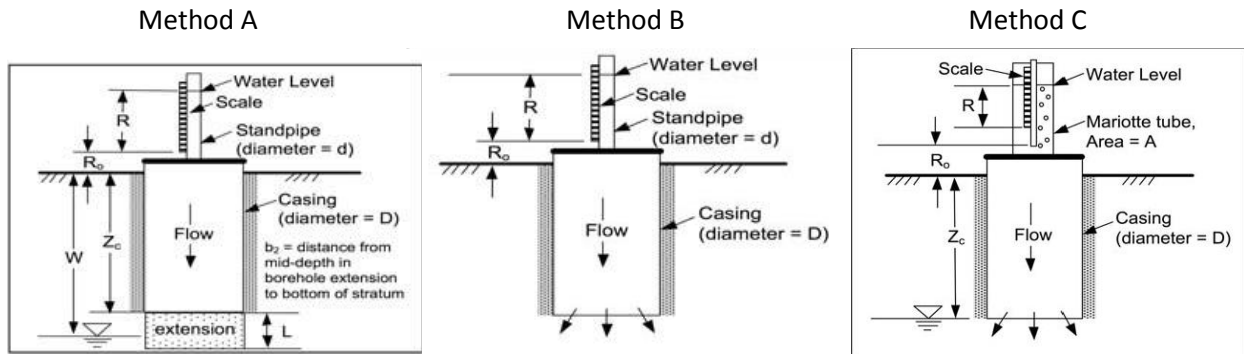


**Fig. 1. Different methods for calculating hydraulic conductivity according to ASTM D6391 (from ASTM D6391 2014).**

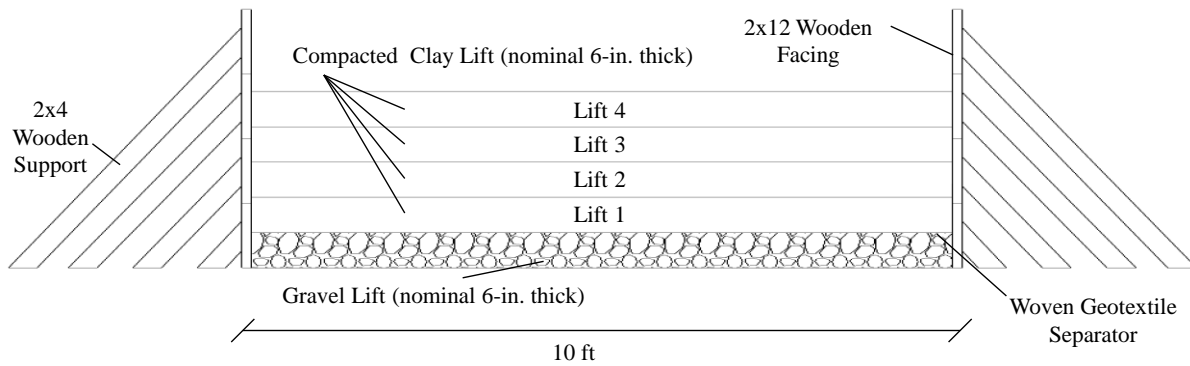


**Fig. 2. Dimensions of test pad box (from Nanak 2013).**

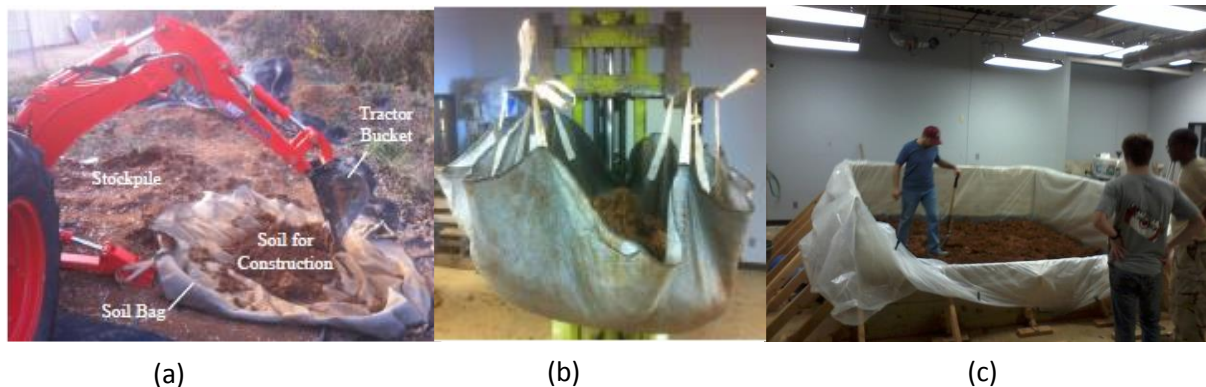


**Fig. 3 (a) Using the tractor to fill the haul bag (Nanak 2013), (b) positioning the haul bag over the box (Nanak 2013), and (c) placing the loose lift of soil (photograph taken by author).**

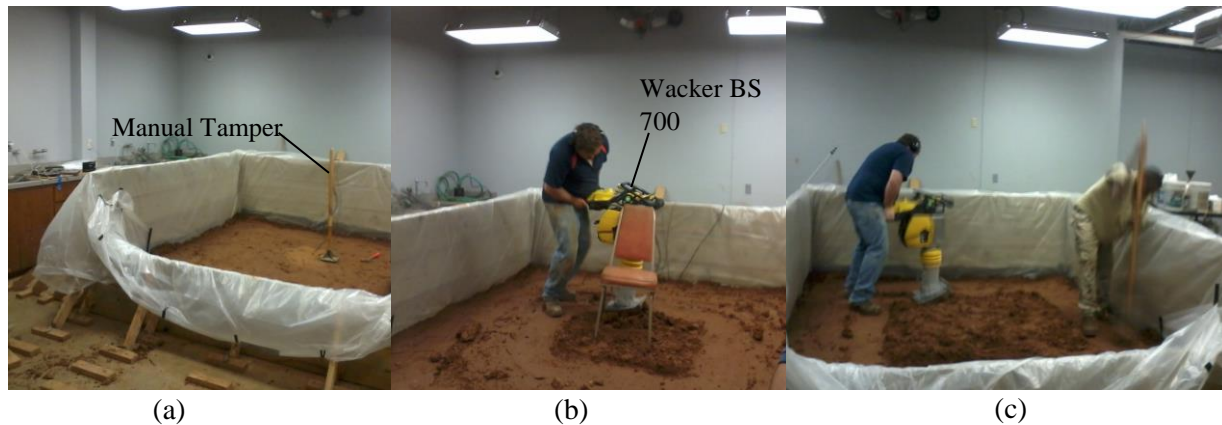


**Fig. 4. (a) Manual tamper on center of pad, (b) Wacker near the center of pad, and (c) compaction of second half of Lift 1 between a depth of 21 inches and 18 inches (photographs taken by author).**

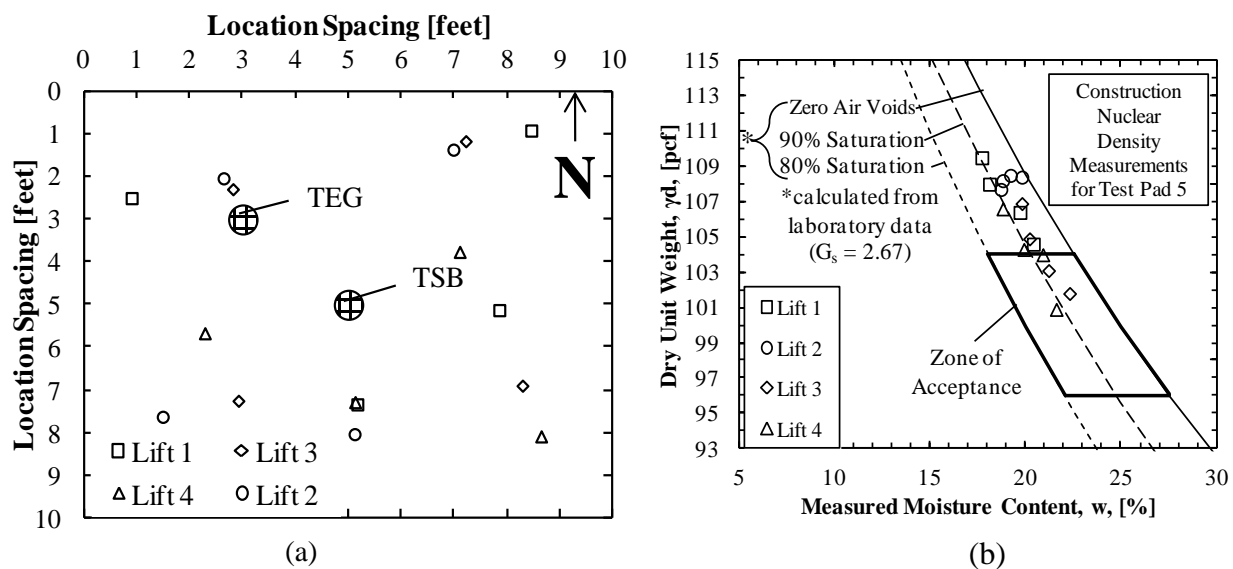
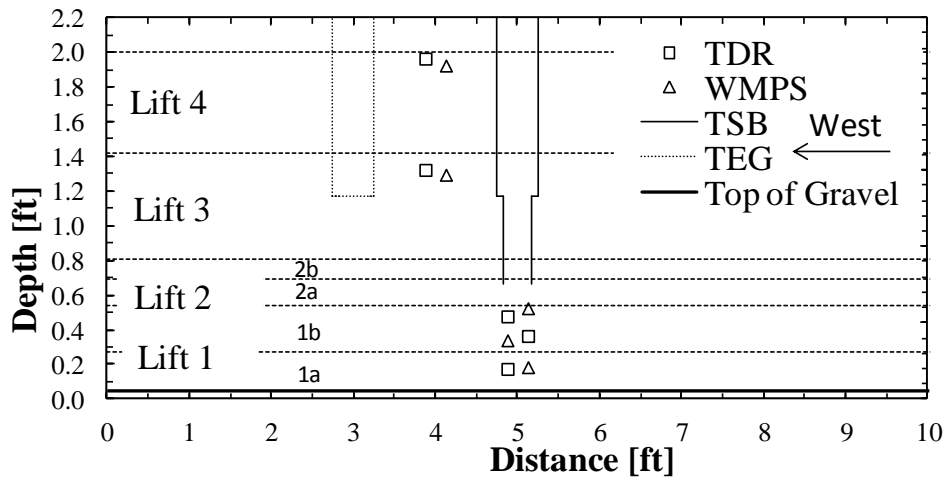


**Fig. 5. (a) Plan view of nuclear density gauge testing location for each lift and (b) results of nuclear density gauge plotted against the zone of acceptance (Test Pad 5 data plotted on ZOA from Nanak 2013).**

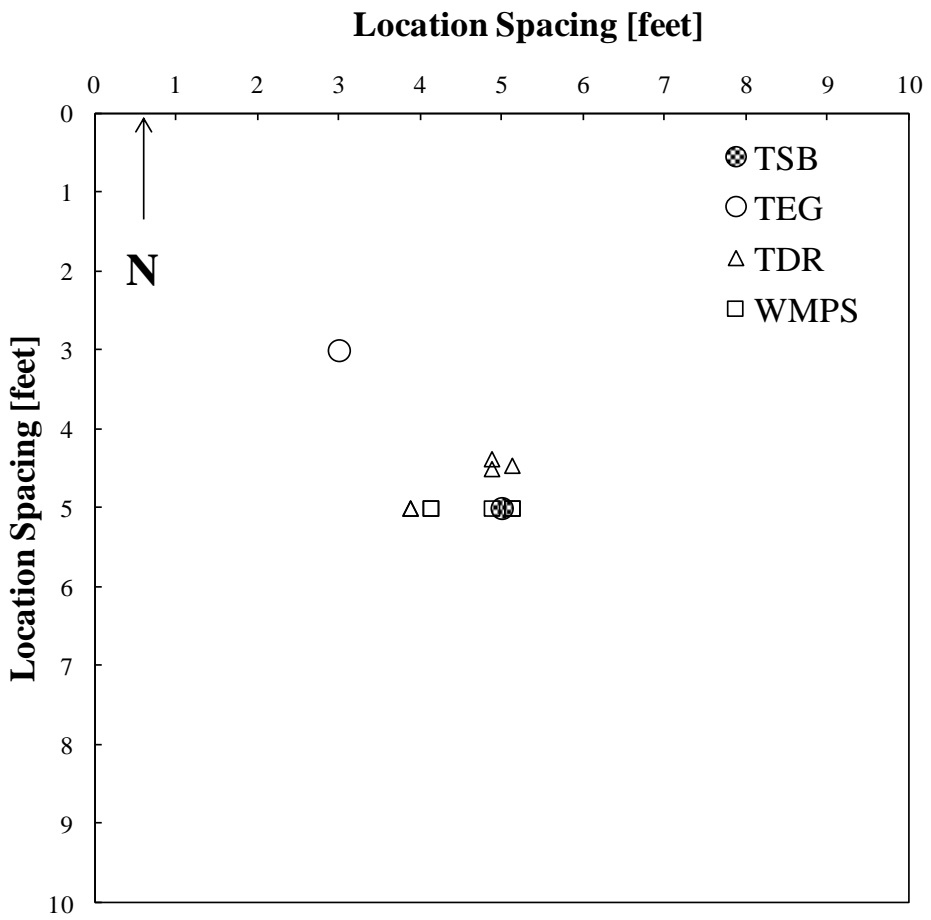




**Fig. 6. Test pad after construction and before TSB testing (photograph taken by author).**



(a)

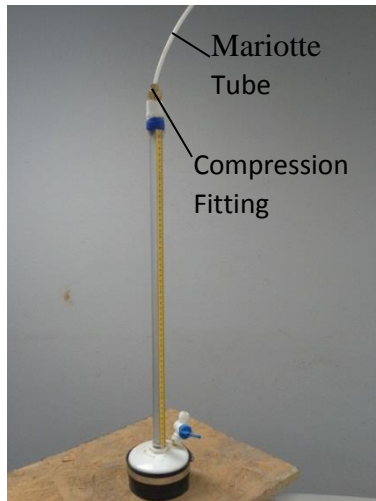


(b)

**Fig. 7 (a) Profile view of test pad and instrumentation and (b) plan view of test pad and instrumentation.**



**Fig. 8. Constant head TSB apparatus and TEG apparatus during testing (photograph taken by author).**



(a)



(b)

**Fig. 9. (a) Constant head TSB apparatus (photograph taken by author) and (b) falling head TSB apparatus during testing (from Nanak 2013).**

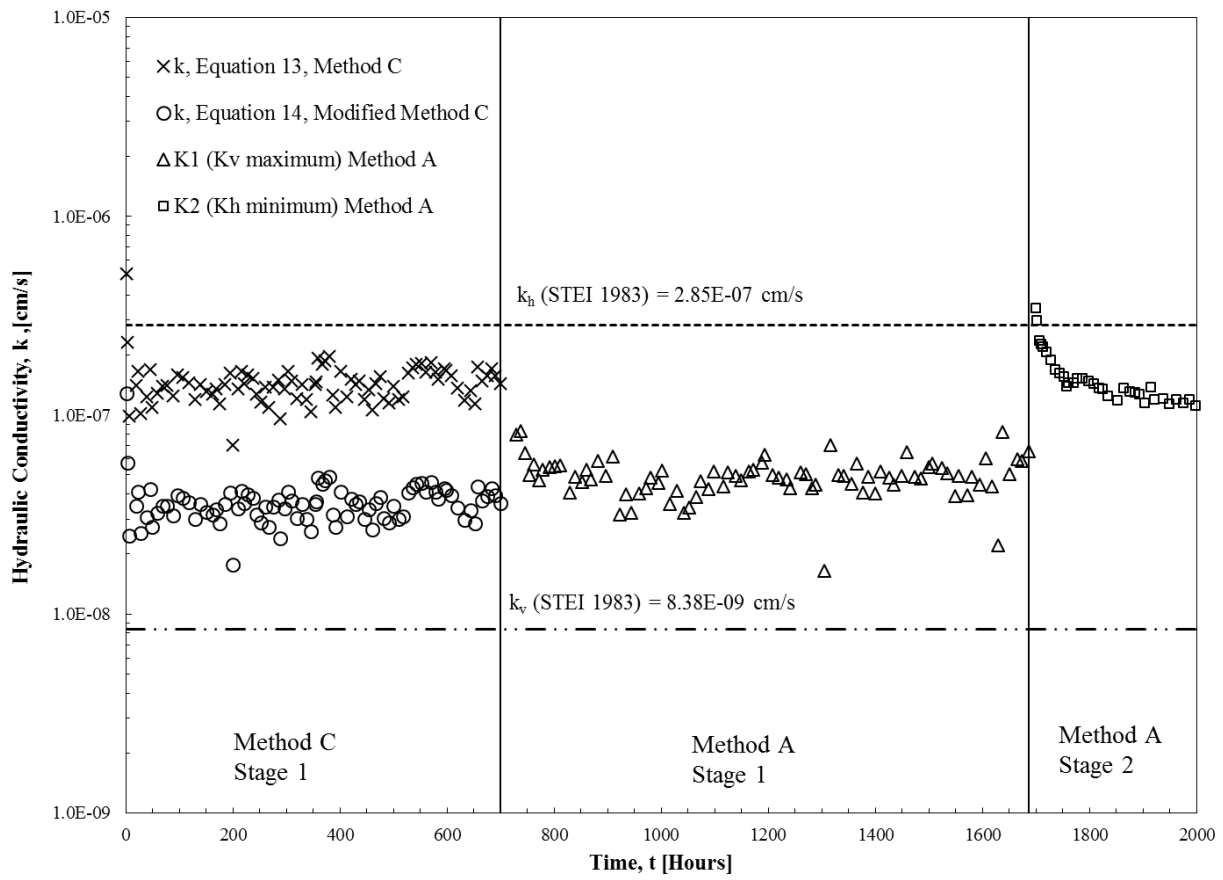
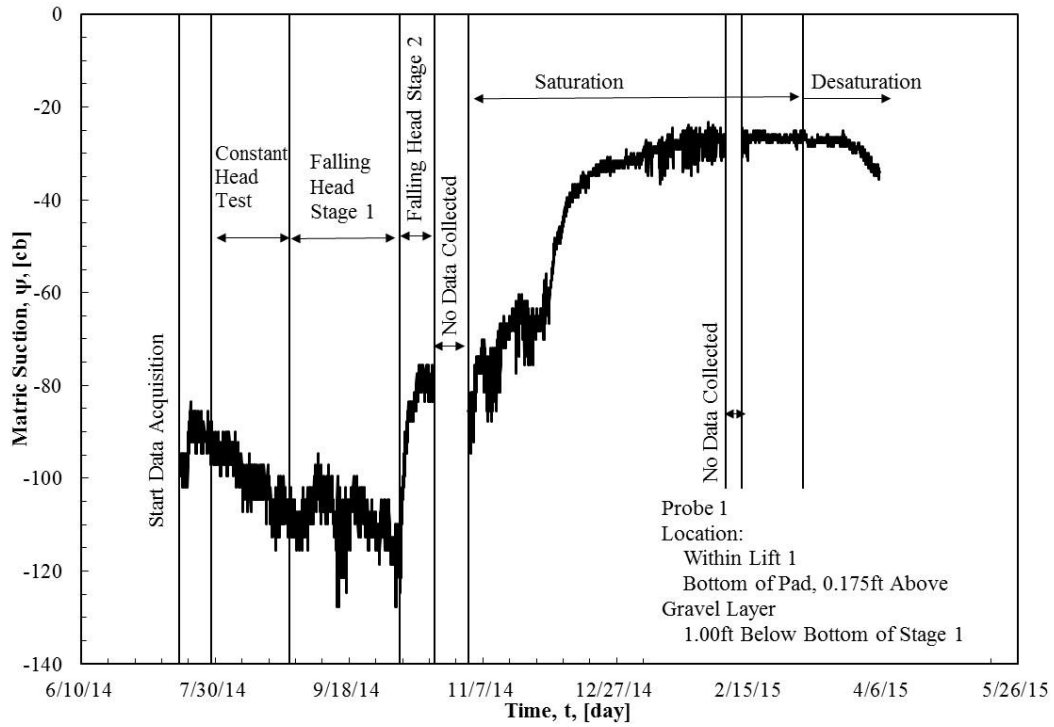


**Fig. 10. Hydraulic conductivity values as a function of time.**



(a)

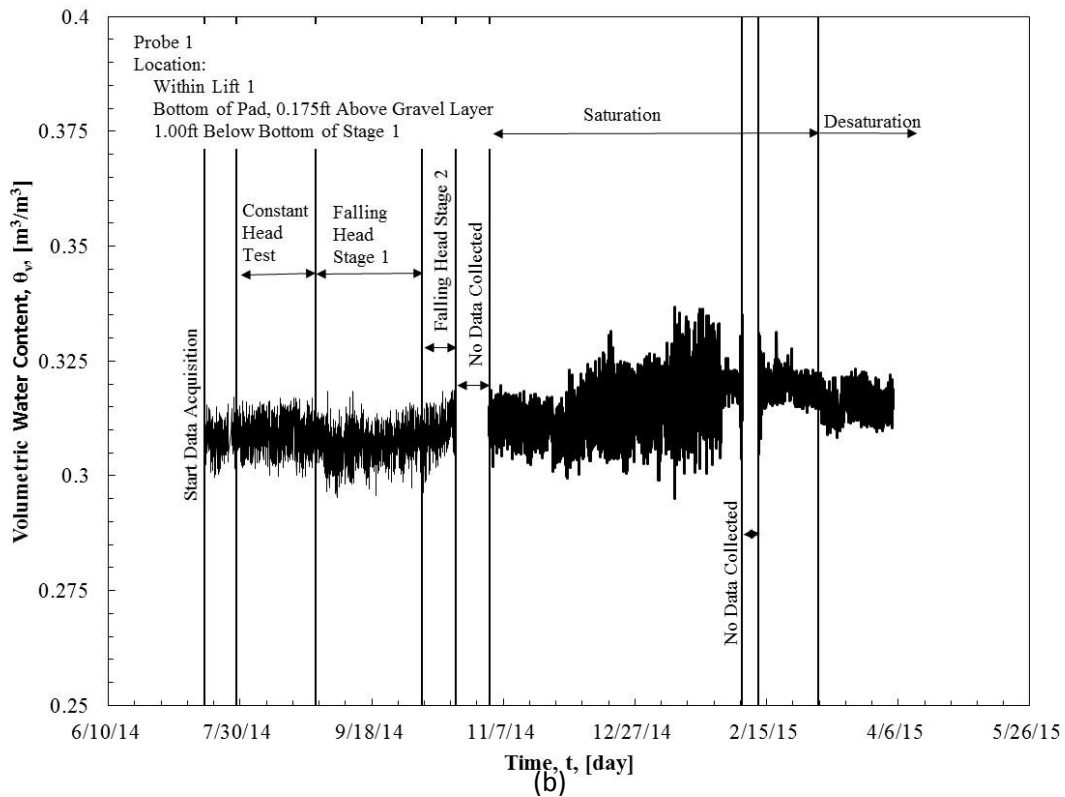
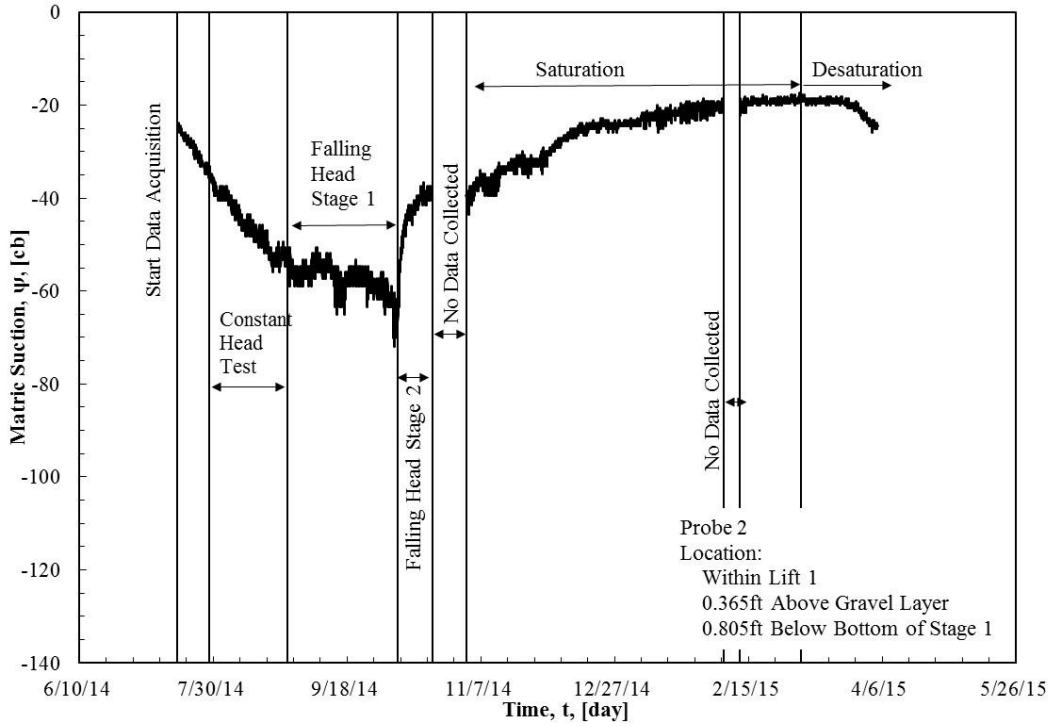
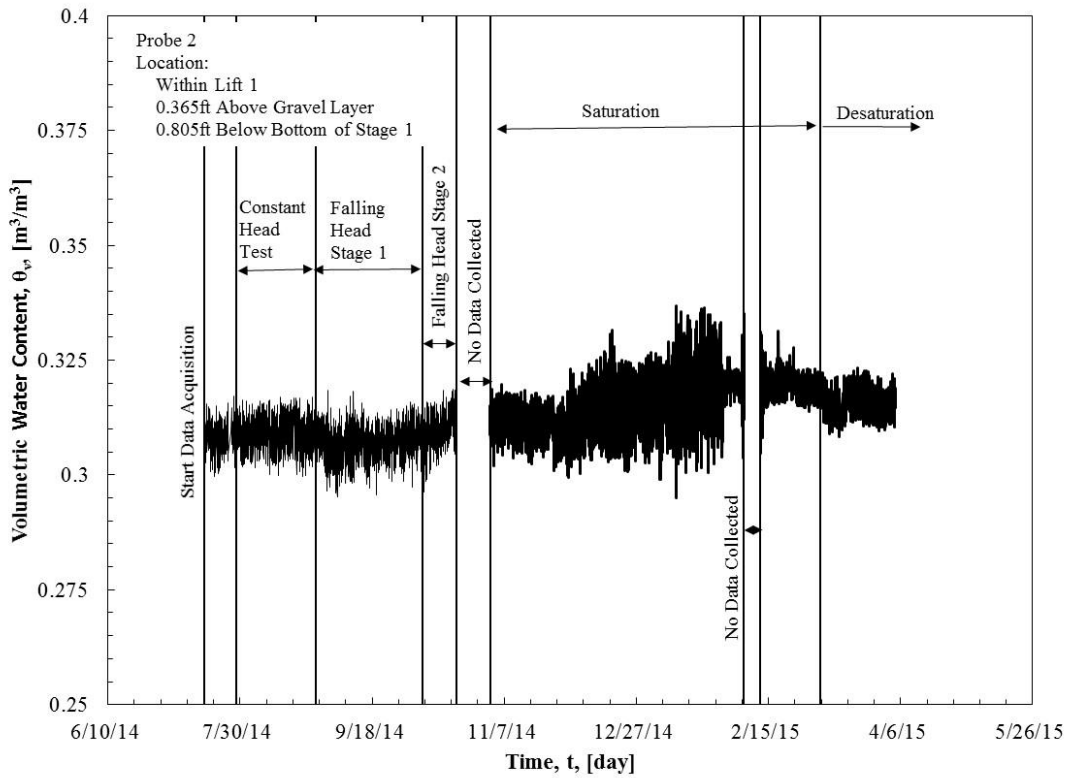


Fig. 11 Matric suction (a) and volumetric water content (b) data from WMP sensor and TDR probe set 1, respectively.



(a)



(b)

**Fig. 12** Matric suction (a) and volumetric water content (b) data from WMP sensor and TDR probe set 2, respectively.

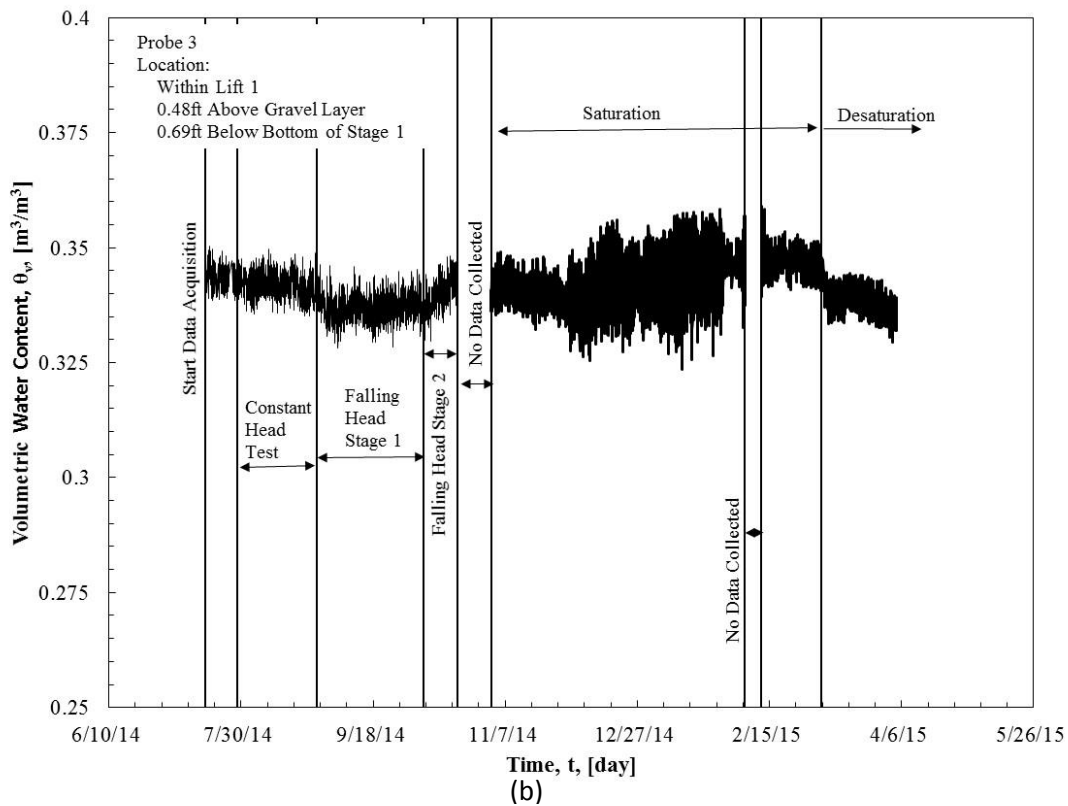
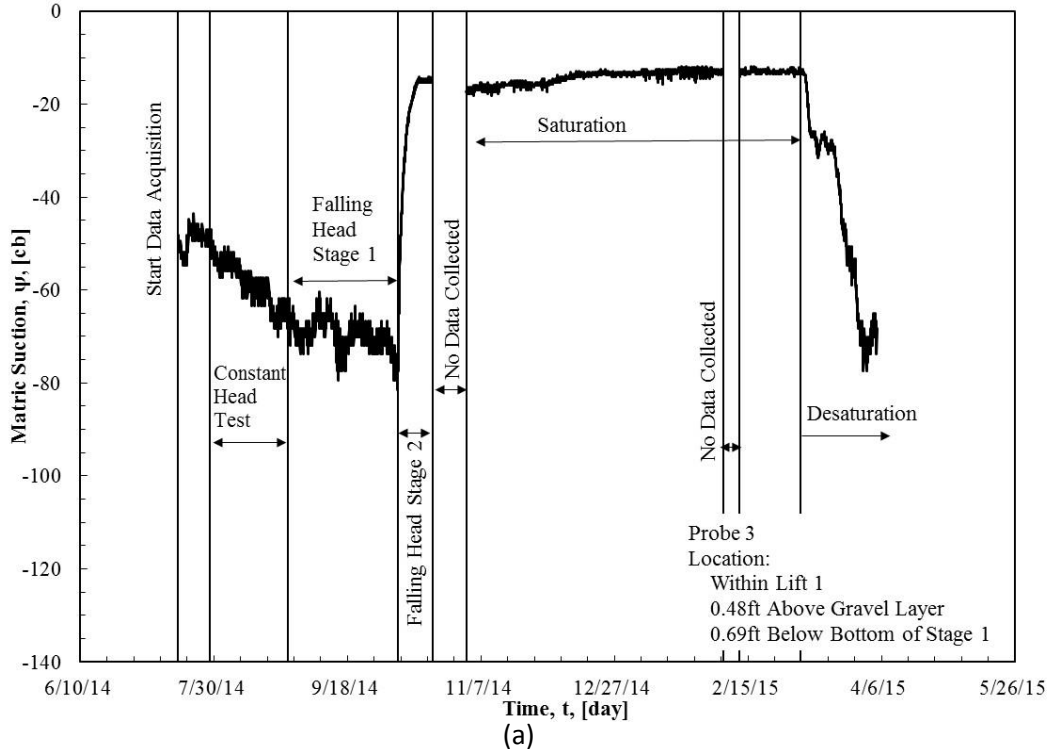
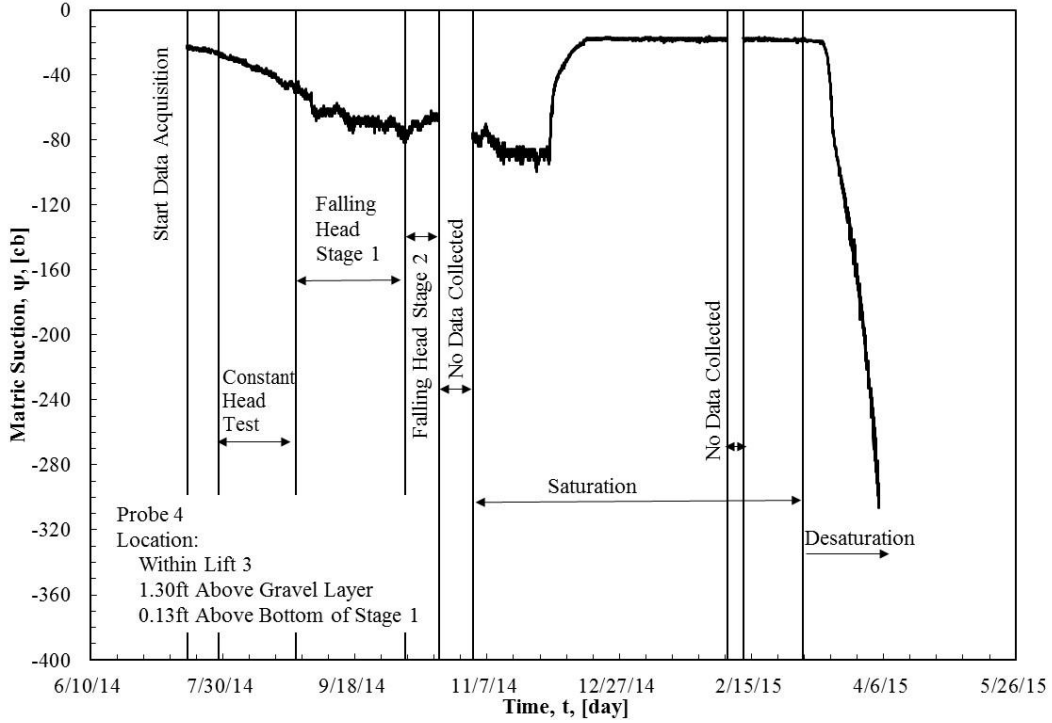
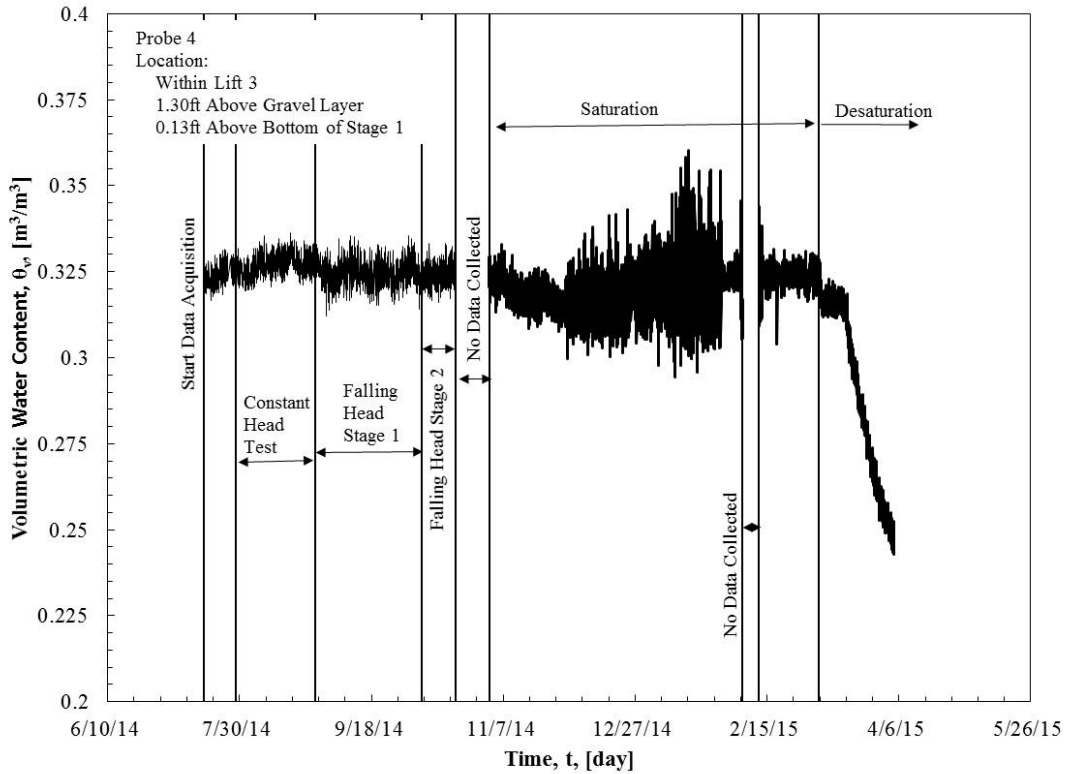


**Fig. 13** Matric suction (a) and volumetric water content (b) data from WMP sensor and TDR probe set 3, respectively.



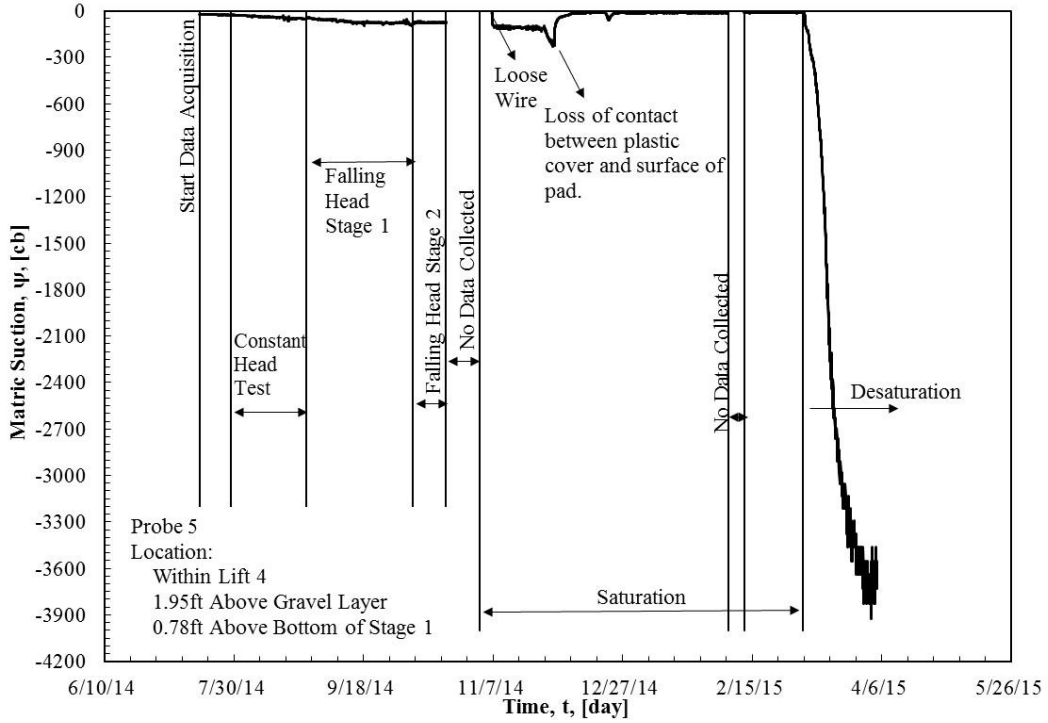
(a)



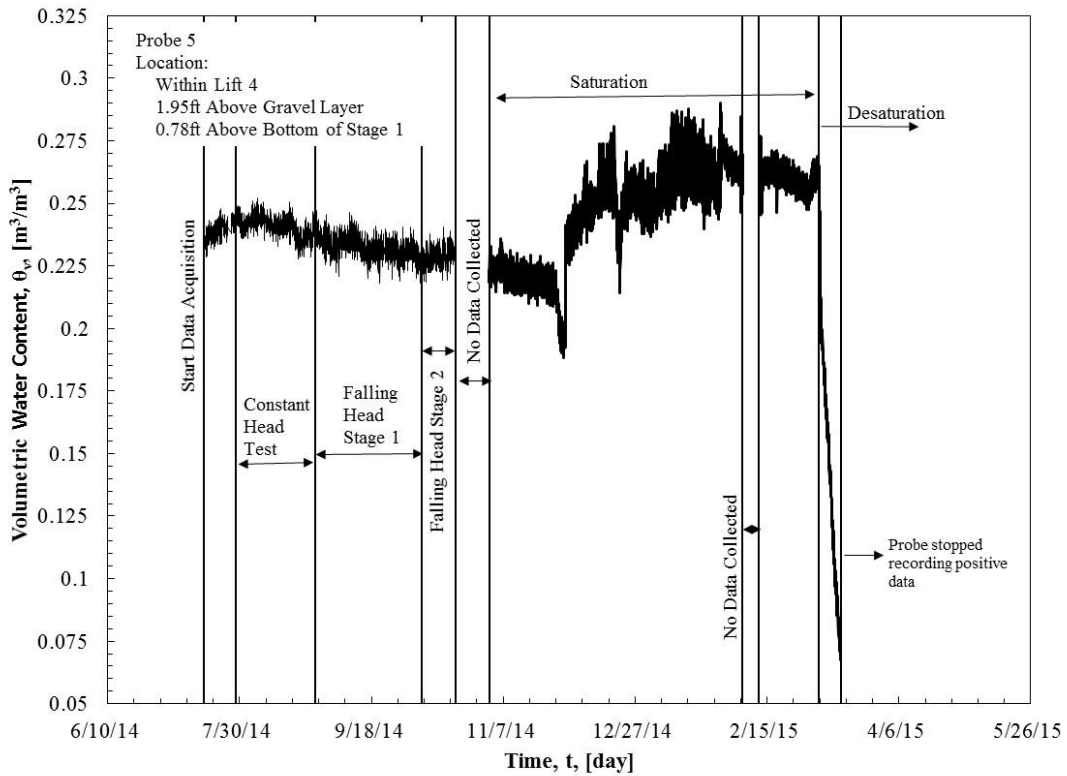
(b)

**Fig. 14** Matric suction (a) and volumetric water content (b) data from WMP sensor and TDR probe set 4, respectively.





(a)



(b)

**Fig. 15 Matric suction and volumetric water content data from WMP sensor and TDR probe set 5, respectively.**

Table 1. Comparison of results from Test Pads 1 & 2 Nanak (2013) and results from Test Pad 5.

	<b>Test Pad 1 Nanak (2013)</b>	<b>Test Pad 2 Nanak (2013)</b>	<b>Test Pad 5</b>
<b>K<sub>1</sub> [cm/sec] (ASTM D6391 2014)</b>	1.09E-08	2.18E-08	4.88E-08
<b>K<sub>2</sub> [cm/sec] (ASTM D6391 2014)</b>	1.50E-08	3.13E-08	1.19E-07
<b>k<sub>v</sub> [cm/sec] (STEI 1983)</b>	5.13E-09	9.41E-09	8.38E-09
<b>k<sub>h</sub> [cm/sec] (STEI 1983)</b>	2.52E-08	5.51E-08	2.85E-07
<b>k<sub>Eq13</sub> [cm/sec] (ASTM D6391 2014)</b>	--	--	1.43E-07
<b>k<sub>Eq14</sub> [cm/sec] (ASTM D6391 2014)</b>	--	--	3.58E-08
<b>k<sub>Lab(HC)avg</sub> [cm/sec] (ASTM D5084 2014)</b>	7.32E-08	3.67E-08	--